Supplementary Figures

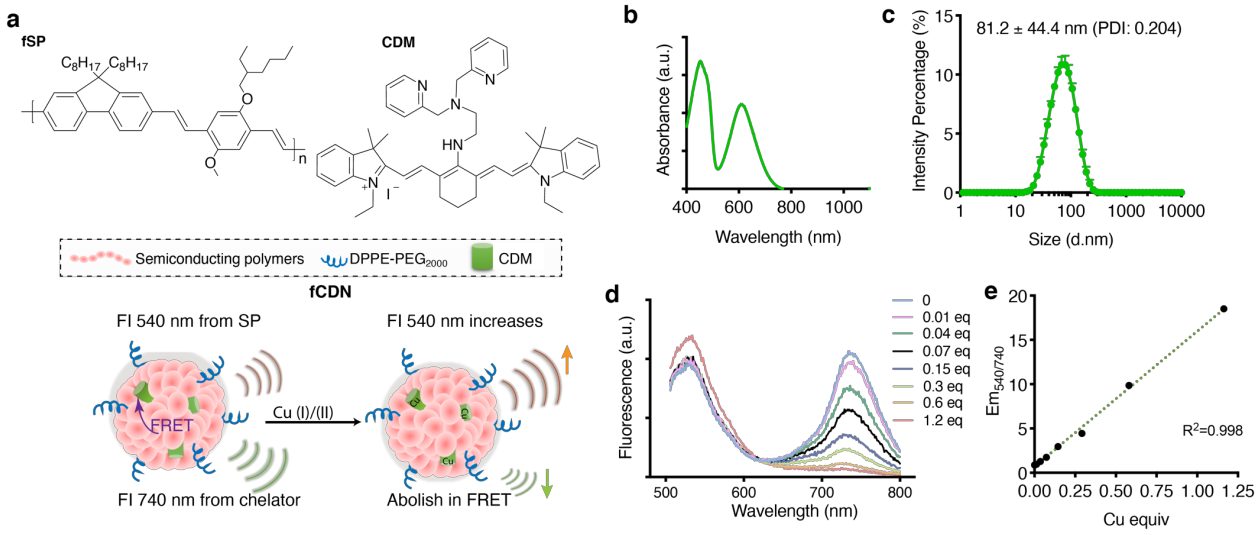

Supplementary Figure 1. Design and characterization of fCDN. (**a**) Molecular components of fCDN and the illustrated nanoparticle formulation. Fluorescent polymer fSP serves as FRET energy donor and CDM serves as energy acceptor. When binding with Cu(I) or Cu(II), the fluorescence of CDM is quenched and the FRET is abolished, resulting in an increase of the polymer signal and decrease of the CDM signal. This ratiometric change depicts the copper binding to fCDN. (**b**) UV-Vis spectrum of fCDN, showing polymer peaks at 453 nm and CDM absorption peaks at 610 nm. (**c**) DLS size measurement of fCDN (mean ± s.d., n=4 independent samples). (**d**) Emission spectra of fCDN upon binding with different equivalents of Cu(II) in solution (Ex: 453 nm). (**e**) Fluorescence ratiometric response of CDN to different equivalents of Cu(II) (Data points were extracted from one set of spectrum measurement).

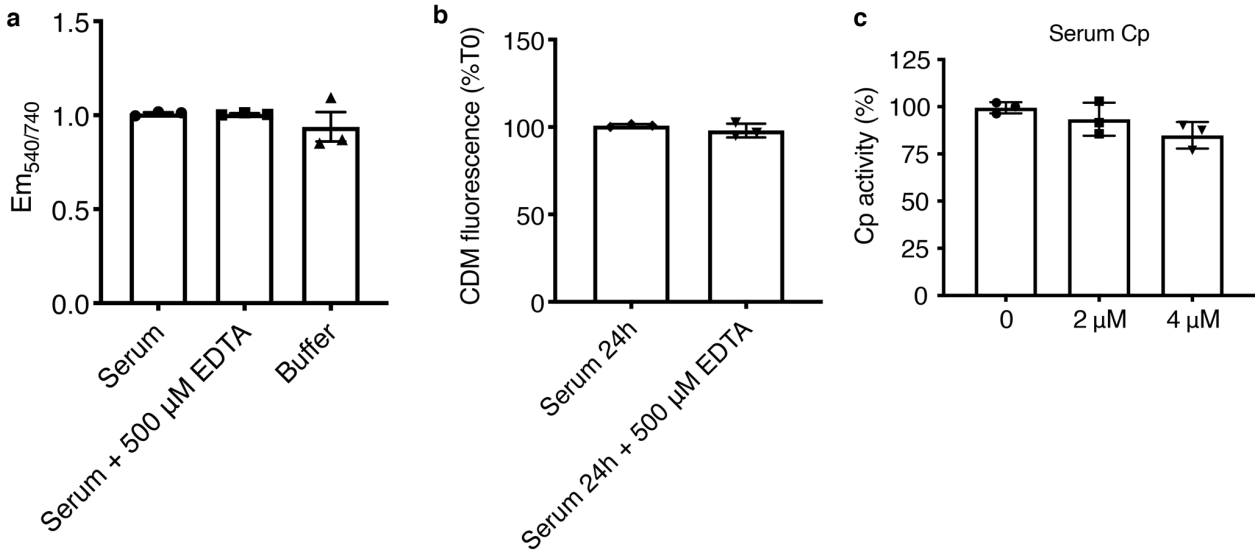

Supplementary Figure 2. Serum stability of CDN. (**a**) Ratio of fluorescence emission intensity at 540 nm and 740 nm of fCDN (Ex: 453 nm, CDM concentration of 1.5 μM) after 24 h incubation with serum with or without 500 μM EDTA for the removal of labile copper or HEPES buffer (10 mM, pH 7.4) at 37 °C (mean ± s.e.m., n=3 independent samples). (**b**) CDM fluorescence intensity when excited at 610 nm after 24 h incubation with serum with or without 500 μM EDTA at 37 °C (mean ± s.e.m., n=3 independent samples). Results are presented as ratio percentage to the intensity before incubation (F_0). (**c**) Ceruloplasmin (Cp) activity in the serum with or without incubation with CDN for 24 h at 37 °C (mean ± s.e.m., n=3 independent samples). Results are presented as ratio percentage to the Cp activity (mU/mL) before incubation.

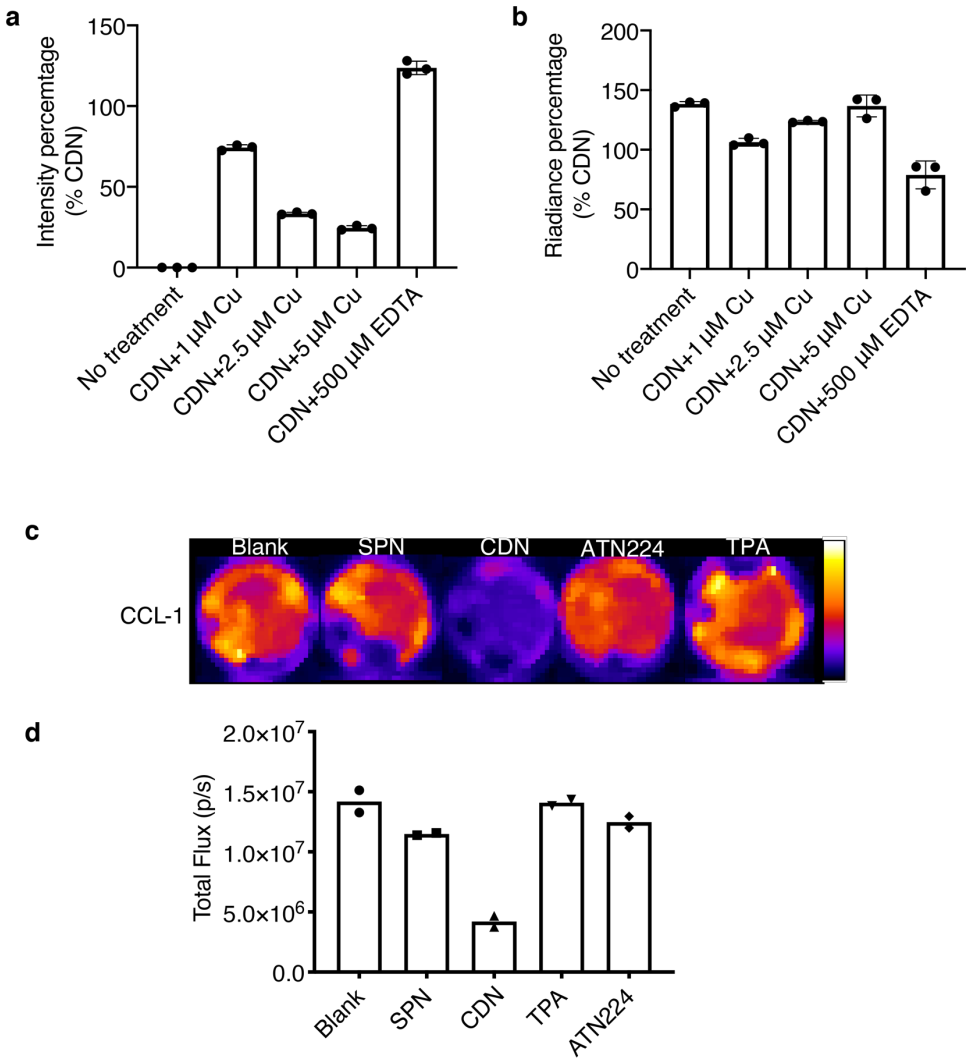

Supplementary Figure 3. Quantification of (**a**) fluorescence and (**b**) luminescence images of MDA-MB-231^{luc} cells after 24 h incubation with CDM with or without different concentrations of copper supplements or excessive EDTA for copper deprivation (CDM: 1 μM). Results were shown as percentage of signal intensity of those in CDN treatment group (mean ± s.d., n=3 independent experiments). (**c**) Representative CCL-1 bioluminescence imaging of 4T1^{luc} cells after 24 h incubation with SPN, CDN, ATN224 or TPA (chelator concentration: 1 μM, SPN concentration: 50 μg/ml). The photon flux is quantified and shown (**d**) (n=2 independent experiments).

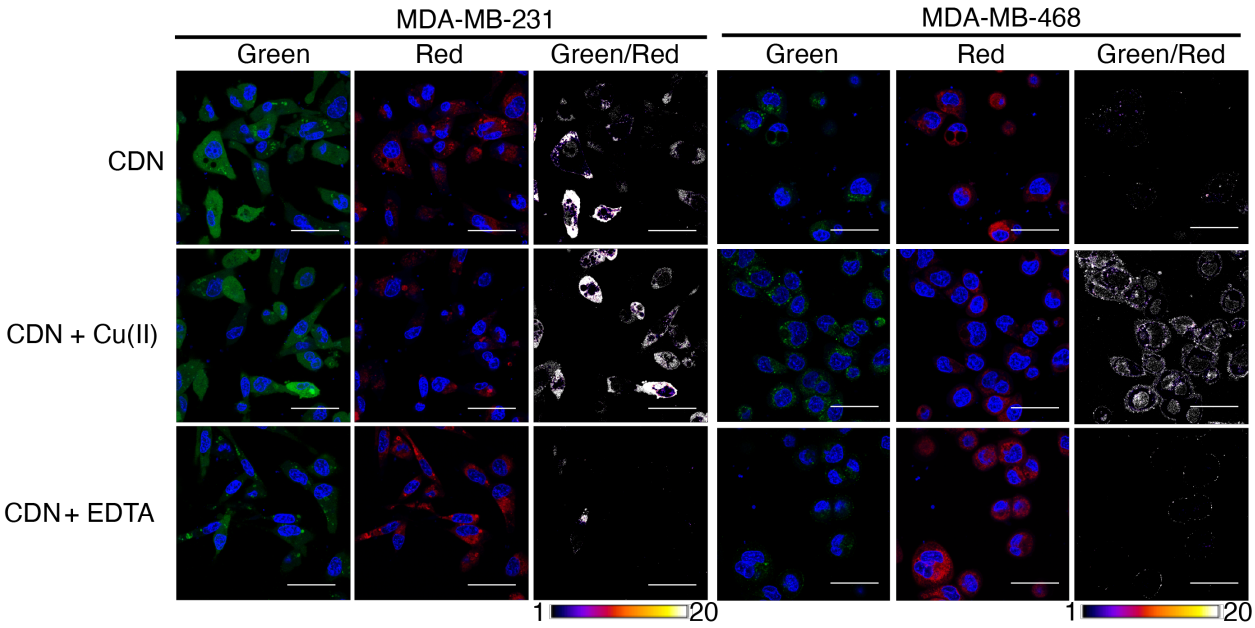

Supplementary Figure 4. Representative confocal microscopy images of MDA-MB-231 and MDA-MB-468 cells after 24 h incubation with fCDN with or without 10 μM of Cu(II) supplement or 500 μM of EDTA (CDM: 1 μM). The green channel shows fluorescence from fSP and the red channel shows the FRET fluorescence from CDM when exciting at 488 nm. The copper content is indicated as the green/red ratio and presented in processed pseudo-colored images. (scale bar: 50 μm) (n=3 independent experiments).

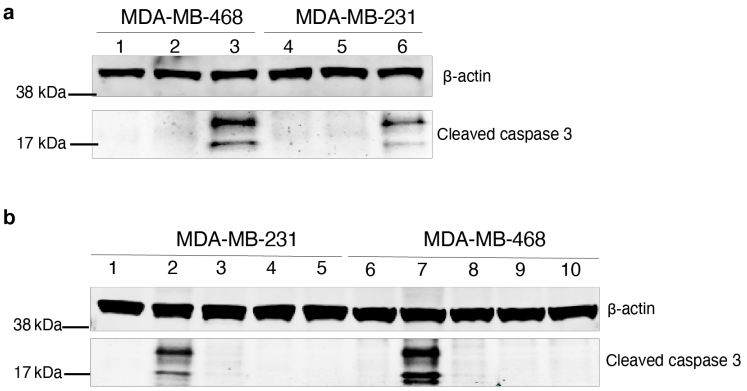

Supplementary Figure 5. (**a**) Cleaved caspase 3 was found after 24 h incubation with CDN (CDM: 1 μM) by western blot analysis, but not with ATN224 treatment (5 μM) in MDA-MB-468 and MDA-MB-231 cells. Lane 1,4: control group without treatment; 2,5: ATN224 group (5 μM); 3,6: CDN group (CDM: 1 μM). Two experiments with were repeated independently with similar results. (**b**) Apoptosis induced by CDN treatment can be rescued with BID inhibitor, BI-6C9. Unlike CDN, IACS 010759 and BAY 872243 did not induce apoptosis of MDA-MB-231 cells at 24 h after incubation at 1 μM concentration. Lane 1,6: control group without treatment; 2,7: CDN group (CDM: 1 μM); 3,8: CDN with BI-6C9 (CDM: 1 μM, BI-6C9: 100 μM); 4, 9: IACS 010759 (1 μM); 5, 10: BAY 87-2243 (1 μM). Two experiments were repeated independently with similar results.

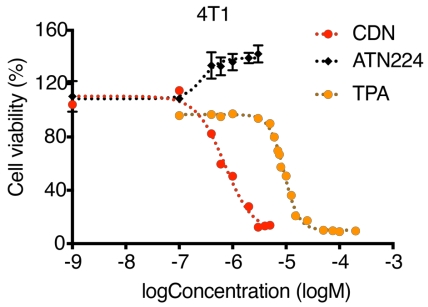

Supplementary Figure 6. 4T1 cell viability (percentage of cell control without treatment) after 24 h incubation with different concentrations of CDN, TPA or ATN224 in complete medium with 10% FBS measured by MTS assay (mean ± s.e.m., n=3 biologically independent samples).

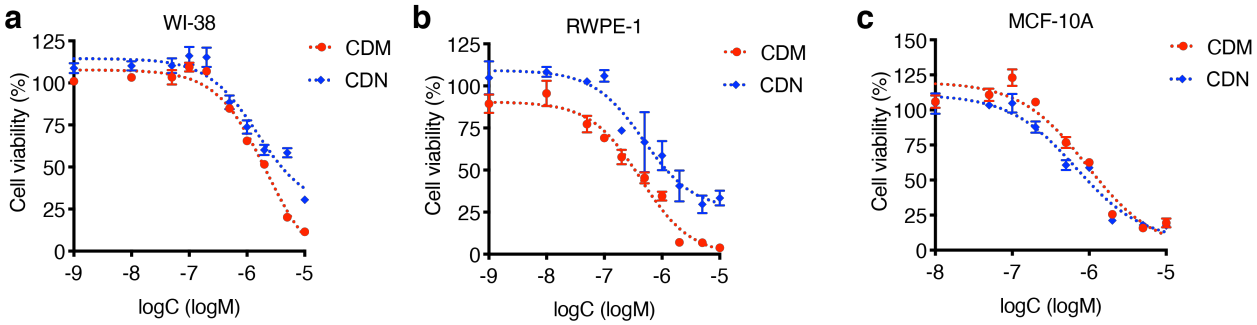

Supplementary Figure 7. (**a**) WI-38, (**b**) RWPE-1 and (**c**) MCF-10A cell viability (percentage of cell control without treatment) after 24 h incubation with different concentrations of CDN or CDM in serum-free medium (supplemented with EGF) measured by MTS assay (mean ± s.e.m., n=3 biologically independent samples).

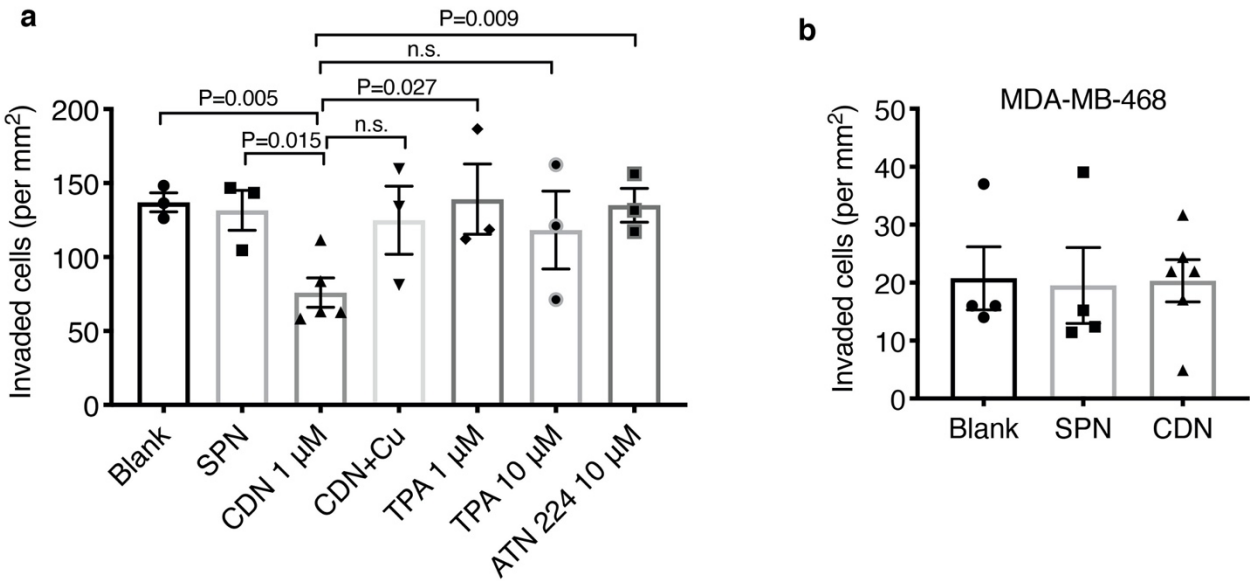

Supplementary Figure 8. Inhibition on the cell invasion upon treatment with various control agents and CDN, determined by Matrigel *in vitro* invasion assay for (**a**) MDA-MB-231 and (**b**) MDA-MB-468 (CDM: 1 μM, SPN: 50 μg/ml). Invaded cell number was normalized by the cell viability measured by MTS study. Data is presented as mean ± s.e.m. (P values from unpaired t test, two-tailed). For MDA-MB-231 cells, n=3 biologically independent samples for blank, SPN, CDN with copper, TPA, and ATN224 group; n=5 biologically independent samples for CDN group. For MDA-MB-468 cells, n=4 biologically independent samples for blank and SPN group; n=5 biologically independent samples for CDN group.

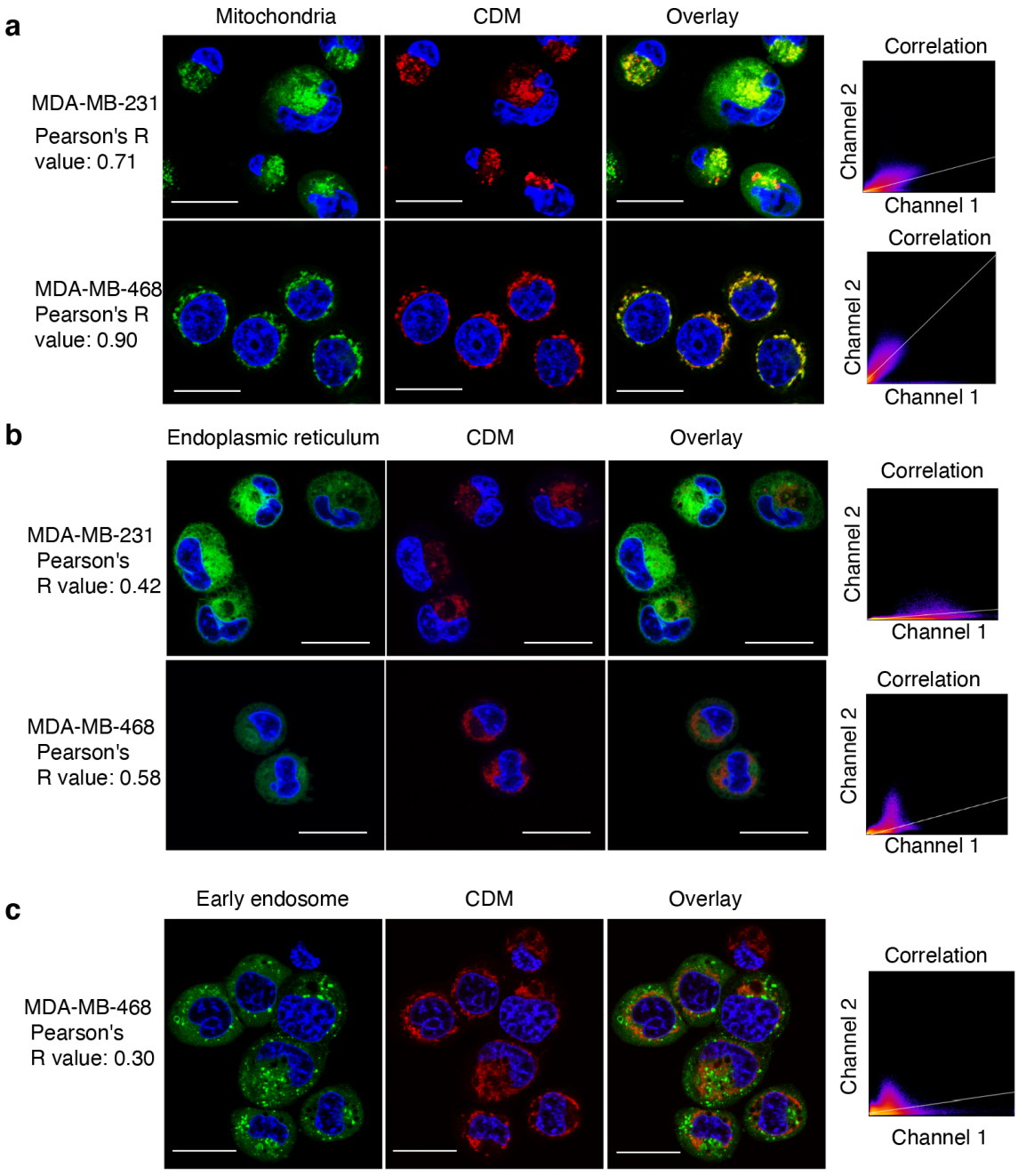

Supplementary Figure 9. Representative subcellular localization of CDN determined by co-staining of organelle and CDN. (**a**) Representative confocal microscopy images of cells co-incubated with Mitotracker (Green) and CDN (CDM: 1 μM, red) for 30 min. (**b**) Representative confocal microscopy images of cells incubated with CDN (CDM: 0.1 μM, 4 h). Cells were then washed with HBSS for 3 times and stained with ER-tracker Green for 30 min. (c) Representative confocal microscopy images of cells incubated with CDN (CDM: 0.1 μM, red) for 1 h. Cells were pre-incubated with CellLight™ Early Endosomes-GFP (Green) (scale bar: 20 μm). Three experiments were repeated independently with similar results.

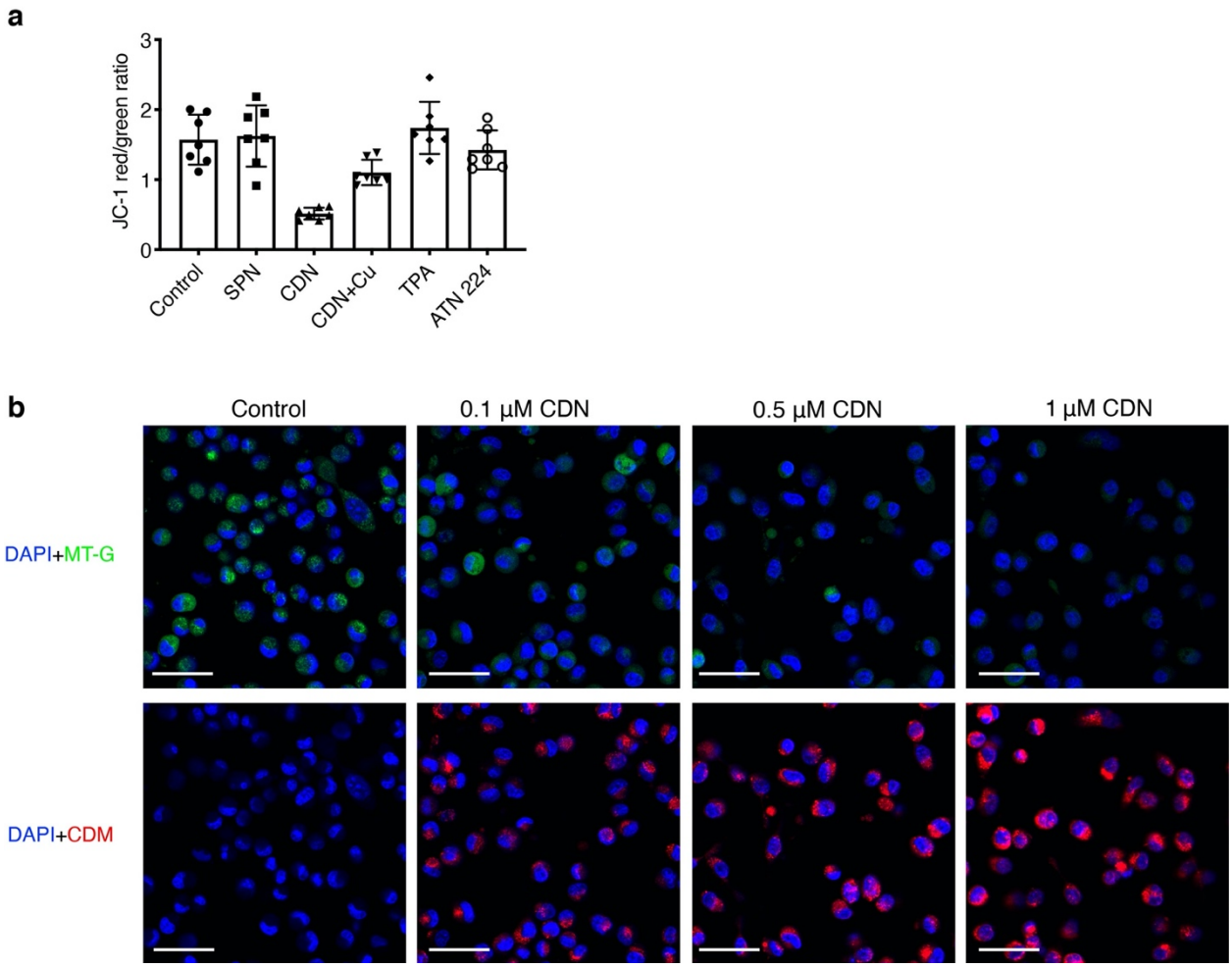

Supplementary Figure 10. (a) Quantification of JC-1 staining in Fig. 3a. JC-1 red signal to green signal ratio of CDN treatment group is significantly lower than control (P<0.0001), SPN (P<0.0001), with copper supplement (P=0.008), TPA (P<0.0001) and ATN224 group (P<0.0001). The ROI analysis was performed out of 7 different views of cells (approximately 50 cells per view) from 3 independent experiments. Results are presented as mean ± s.e.m.; P value was from unpaired t test, two-tailed. **(b)** Mitotracker staining experiment showing that mitochondrial membrane integrity was compromised after CDN treatment. MDA-MB-231 was incubated with different concentrations of CDN for 24 h then stained with Mitotracker Green (Green: MT-G) and DAPI (blue) (Scale bar: 50 μm). Experiments were repeated twice independently with similar results.

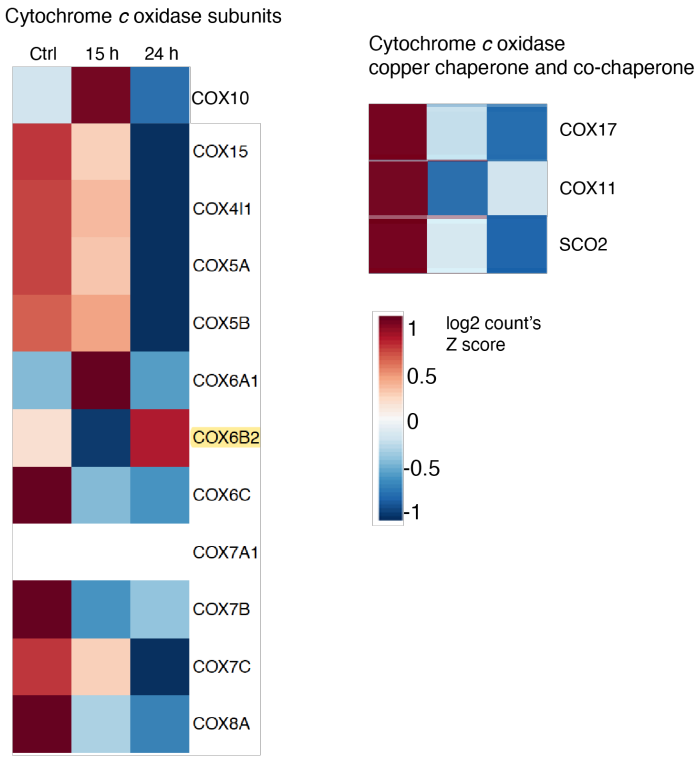

Supplementary Figure 11. mRNA sequencing results showing a major downregulation of gene sets for the subunits of cytochrome c oxidase (except for COX6B2 at 15 h) and its copper chaperone and co-chaperone proteins after treatment with CDN (1 μM).

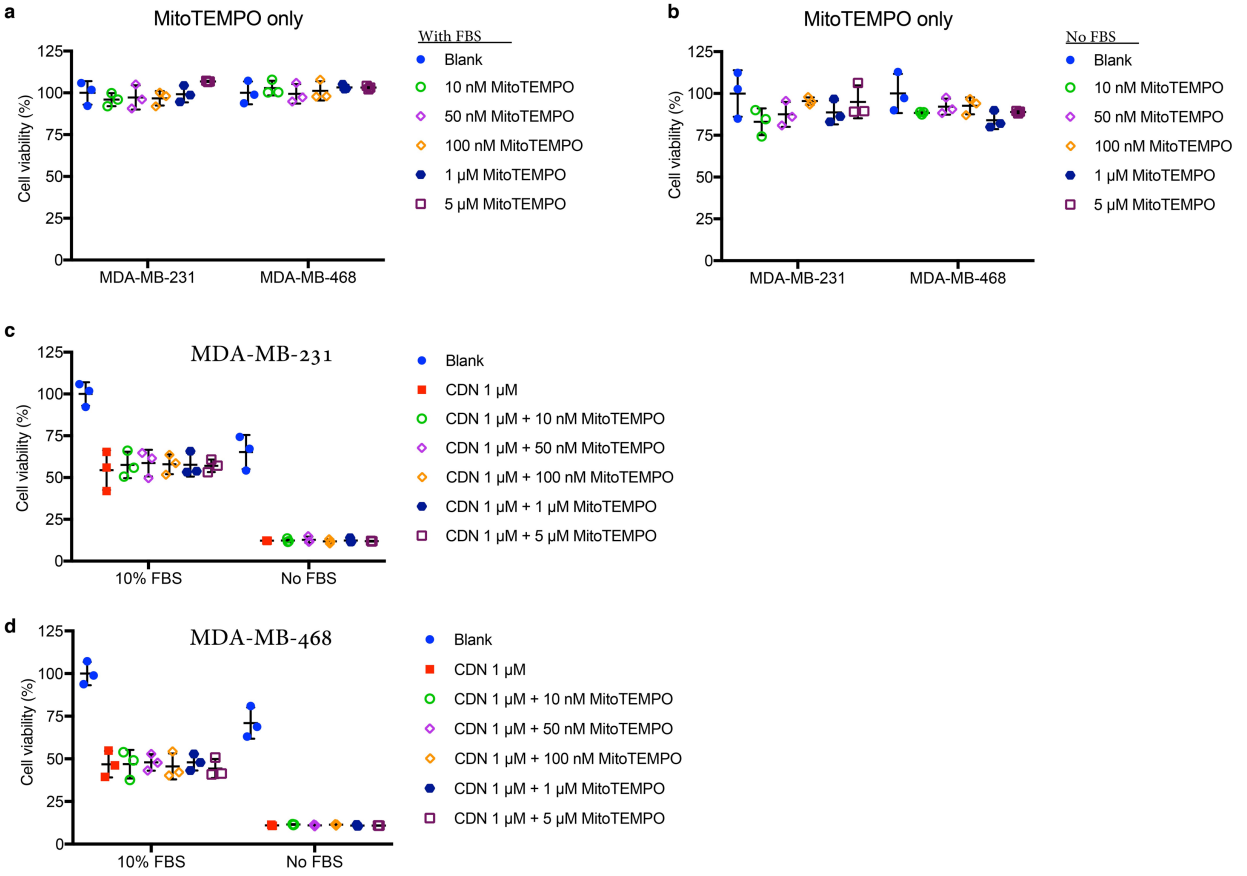

Supplementary Figure 12. Addition of MitoTEMPO up to 5 μM will not affect the cell viability of MDA-MB-231 and MDA-MB-468 cells in medium (**a**) with or (**b**) without FBS supplement. When co-incubation with CDN (CDM: 1 μM) for 24 h, addition of MitoTEMPO did not rescue (**c**) MDA-MB-231 or (**d**) MDA-MB-468 cells in medium with or without FBS supplement. (mean ± s.e.m., n=3 biologically independent samples)

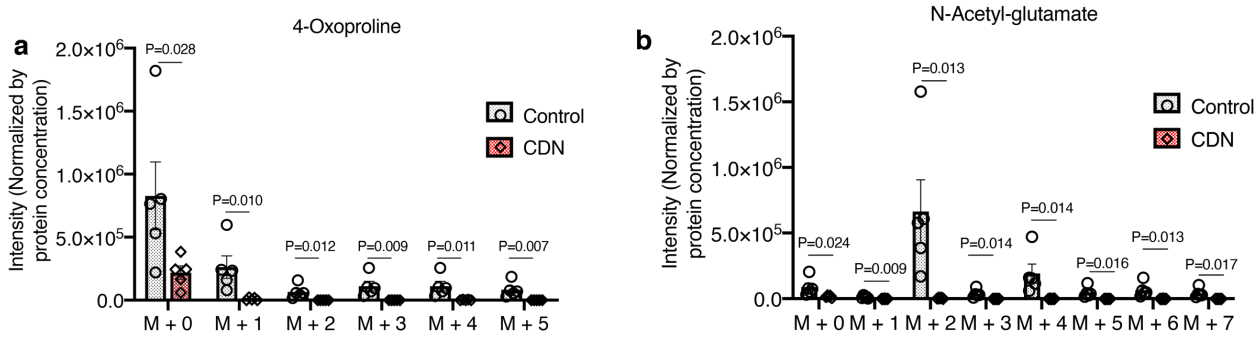

Supplementary Figure 13. Intensities of isotopologues of metabolites, (**a**) 4-oxoproline, (**b**) N-acetyl-glutamate, produced from $^{13}C_6$-labeled glucose *in vitro.* Raw intensities are normalized by protein concentration. Data are shown as mean ± s.e.m. (n=5 biologically independent samples; P values from unpaired t test, two-tailed).

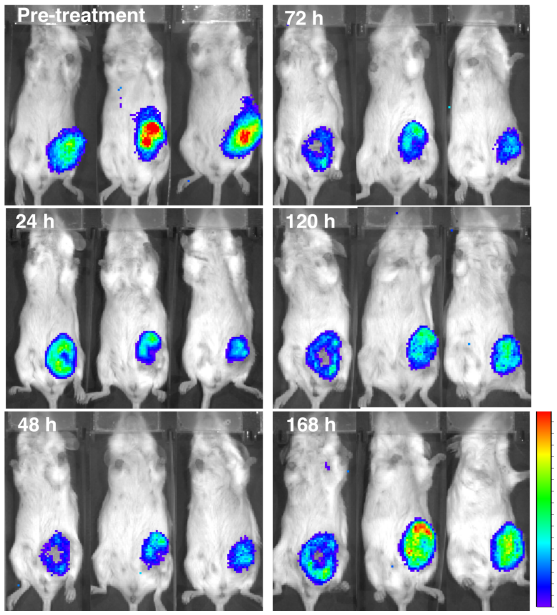

Supplementary Figure 14. Labile copper concentration detected by CCL-1 bioluminescence imaging after *i.v.* injection of CDN (1.35 mg/kg) in MDA-MB-231^{luc} tumor-bearing mice. At each time point, mice were intraperitoneally injected with CCL-1 (6 mg/kg) and imaged with IVIS Spectrum.

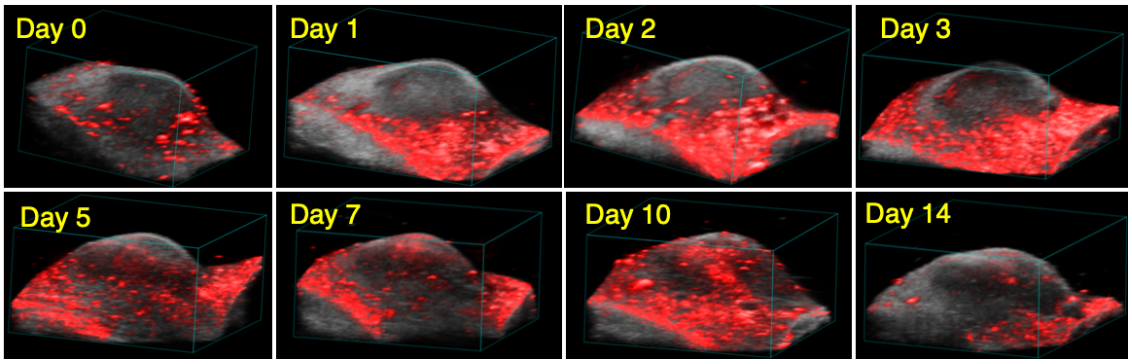

Supplementary Figure 15. Representative 3D reconstruction of the tumor region (grey: B mode ultrasound, red: photoacoustic at 1100 nm) at different time points after *i.v.* injection of CDN (1.35 mg/kg) in MDA-MB-231 tumor-bearing mice.

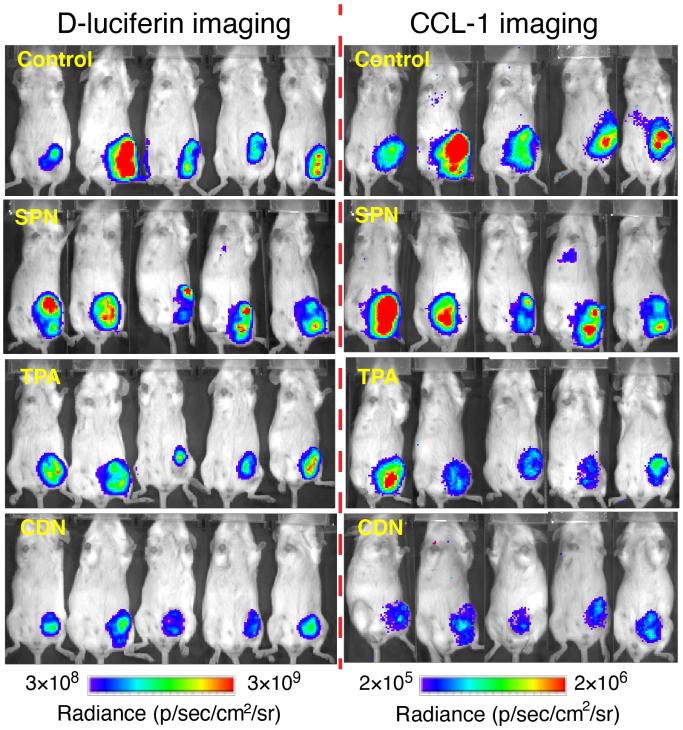

Supplementary Figure 16. D-luciferin and CCL-1 bioluminescence imaging of mice in different treatment groups at day 25 after the first injection. MDA-MB-231^{luc} tumor-bearing mice were divided into four groups: control, SPN control, TPA and CDN (n=5 mice for each group). TPA and CDN group receive *i.v.* injection (chelator dose: 1.35 mg/kg) every three days with a total of five doses. Mice in SPN group received same SPN dose as the CDN group.

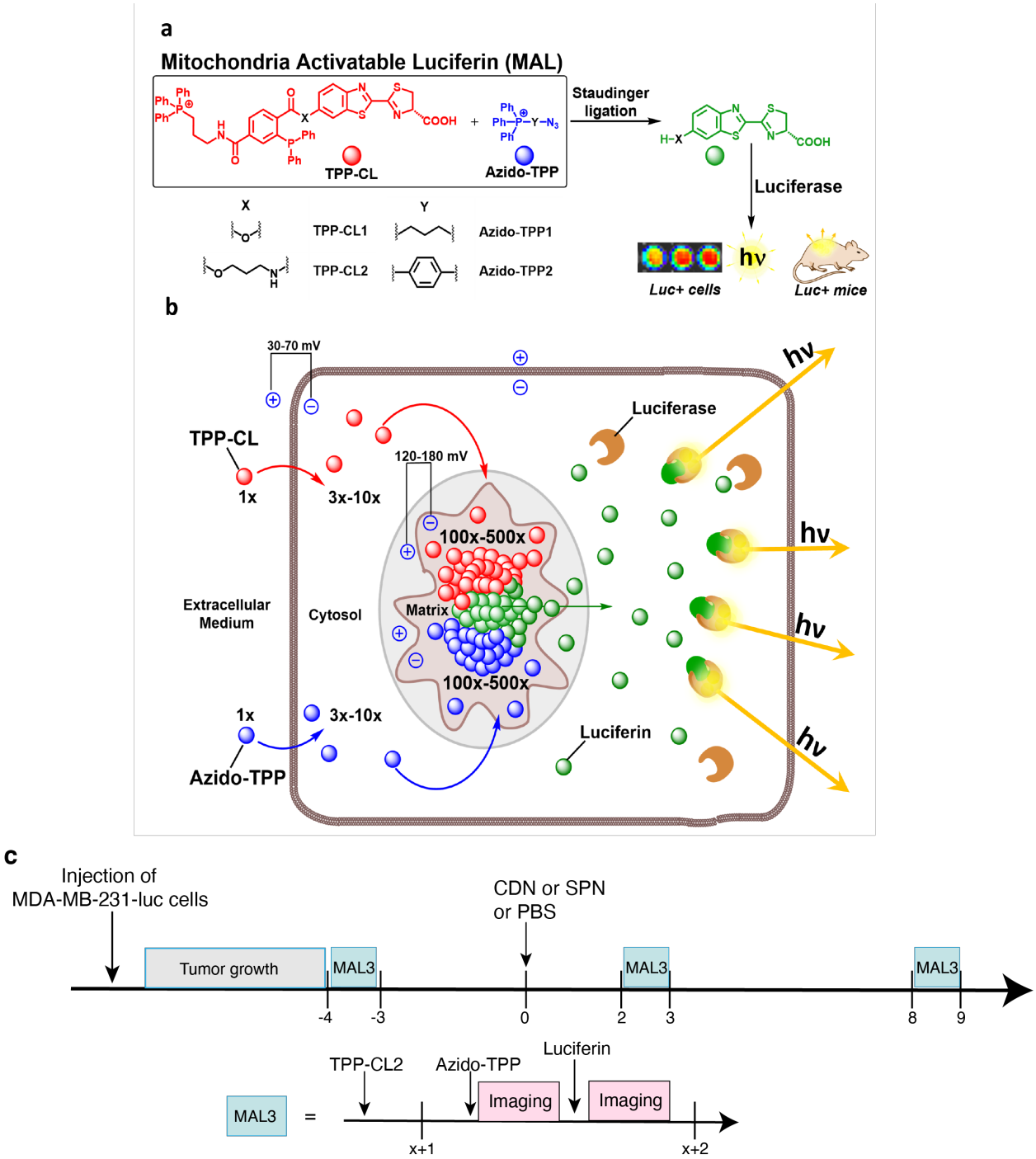

Supplementary Figure 17. Effect of copper depletion on mitochondrial membrane potential (ΔΨm) of MDA-MB-231^{luc} tumor xenografts measured with bioluminescent ΔΨm-specific MAL3 probe. (**a-b**) Design of the mitochondrial-activated luciferin (MAL) probe. The MAL probe consists of two components, a triphenylphosphine-caged luciferin probe (TPP-CL, red-colored ball) and an azido-triphenylphosphine reagent (azido-TPP, blue-colored ball), both of which are targeted to mitochondria because of the triphenylphosphine (TPP) group, similar to other compounds widely used for selective delivering of small molecules to mitochondria. The “click” reaction (Staudinger ligation) between the reagents results in the uncaging of a luciferin derivative (green-colored ball) that in the presence of luciferase results in production of photon flux that can be imaged and

quantified by a CCD camera or standard plate reader. This technology is easily applicable for noninvasive imaging and monitoring of small changes in ΔΨm both in vitro and in vivo in a longitudinal fashion. (**a**) Chemical reaction of MAL components. (**b**) Theoretical illustration of the cellular distribution of MAL reagents in different cellular compartments (extracellular - 1x; cytosolic - 3x-10x; mitochondrial matrix - 100x-500x). (**c**) Timeline of the experiment. On day 0 mice received *i.v.* injection of either CDN, SPN, or PBS (n=5 independent mice). MAL3 probe consists of TPP-CL2 and AzidoTPP1 reagents that are injected sequentially with a 20 h interval. The size of the tumors was assessed by injection of concentrated solution of luciferin right after imaging with MAL3.

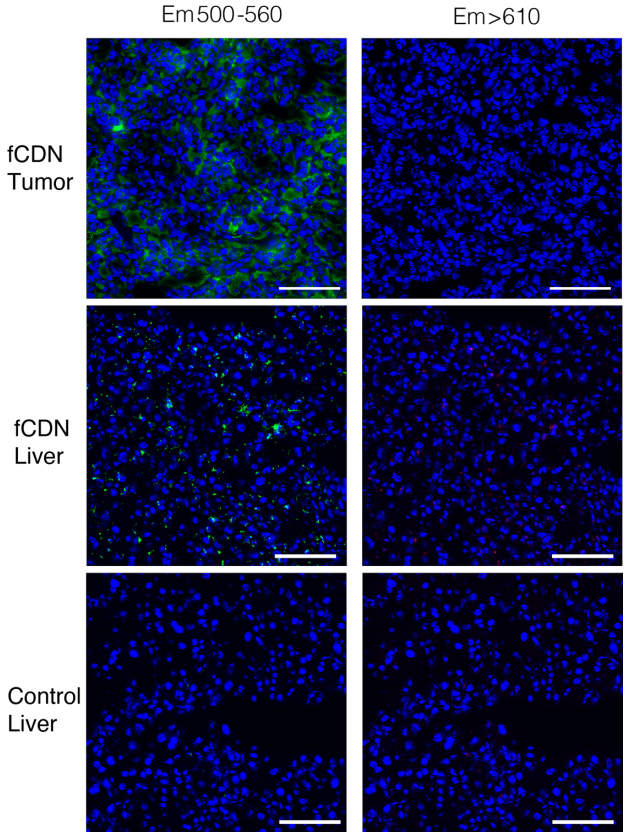

Supplementary Figure 18. Representative confocal microscopy images of tumor and liver slices from control and fCDN administered (CDM dose: 1.35 mg/kg) MDA-MB-231 tumor bearing mice (scale bar: 100 μm). Slices from 6 independent animals were imaged and showed similar results.

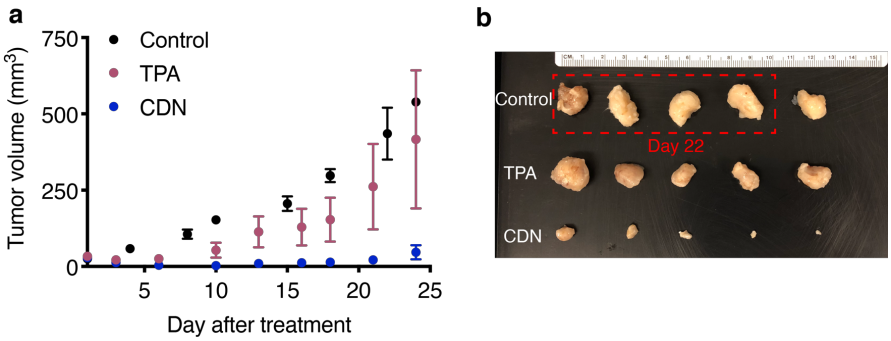

Supplementary Figure 19. (**a**) Tumor growth curve of 4T1 tumor bearing mice in different treatment groups. Data are shown as mean ± s.e.m. (n=5 independent animals). (**b**) Photograph of tumors harvested at day 32 after initial treatment (four tumors in the blank control group were harvested at day 22 due to the large sizes). For the treatment plan, 4T1 tumor bearing mice were divided into three groups: control, TPA and CDN (n=5 mice for each group). TPA and CDN groups received *i.v.* injection (chelator dose: 1.35 mg/kg) weekly days with a total of five doses.

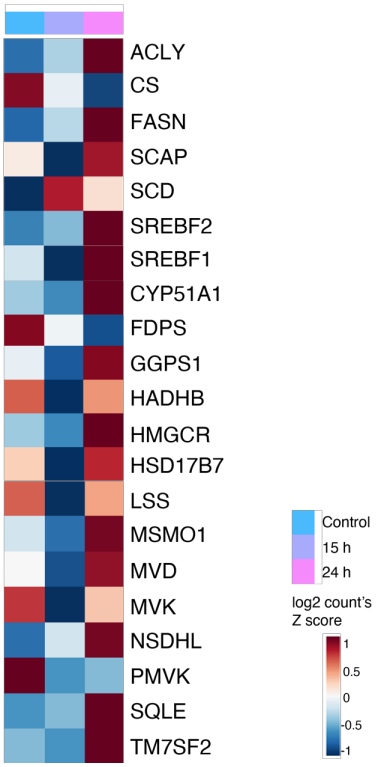

Supplementary Figure 20. mRNA sequencing results showing a major upregulation of gene sets involved in fatty acid synthesis and cholesterol synthesis after 24 h treatment with CDN. All measurements were taken from distinct samples.

Supplementary Notes

CDM synthesis. CDM was prepared according to reported procedures with some modifications (J. Am. Chem. Soc. 2006, **128**, 6548–6549).

(1) Synthesis of compound **3**. N-Boc-Ethylenediamine (0.8 g, 5 mmol), Na_2CO_3 (2.4 g, 22.6 mmol), and 2-chloromethylpyridine hydrochloride (1.8 g, 10.9 mmol) were dissolved in methanol and refluxed under argon for 48 h. Then the solvent was evaporated. The residue was dissolved in 1N NaOH solution and extracted by dichloromethane (DCM). The organic phase was dried by anhydrous sodium sulfate and evaporated to give a yellow liquid that was purified by chromatography (Al_2O_3, DCM/MeOH) to afford **2**. Compound **2** (519 mg, 1.508 mmol) was dissolved in DCM to which 3 mL of trifluoroacetic acid was added dropwise on an ice bath. The mixture was stirred under room temperature for 3 h before 1 N NaOH was added to neutralize the solution. The organic phase was dried by anhydrous sodium sulfate and evaporated to get a yellow liquid **3** (335 mg, yield 92 %). ^{1}H NMR (300 MHz, $CDCl_3$): δ 1.92 (s, 2H), 2.67 (t, 2H, J = 5.7 Hz), 2.80 (t, 2H, J = 5.7 Hz), 3.85 (s, 4H), 7.12 (m, 2H), 7.49 (d, 2H, J = 7.7 Hz), 7.63 (td, 2H, J = 7.7 Hz, 1.83 Hz), 8.52 (dd, 2H, J = 4.9 Hz, 0.8 Hz). ^{13}C NMR (75 MHz, $CDCl_3$): δ 39.1, 56.7, 60.1, 121.5, 122.5, 135.9, 148.5, 159.1. MS (ESI$^+$): m/z calculated for $C_{14}H_{18}N_4^+$: calculated 243.1; found 243.2 $(M+H)^+$.

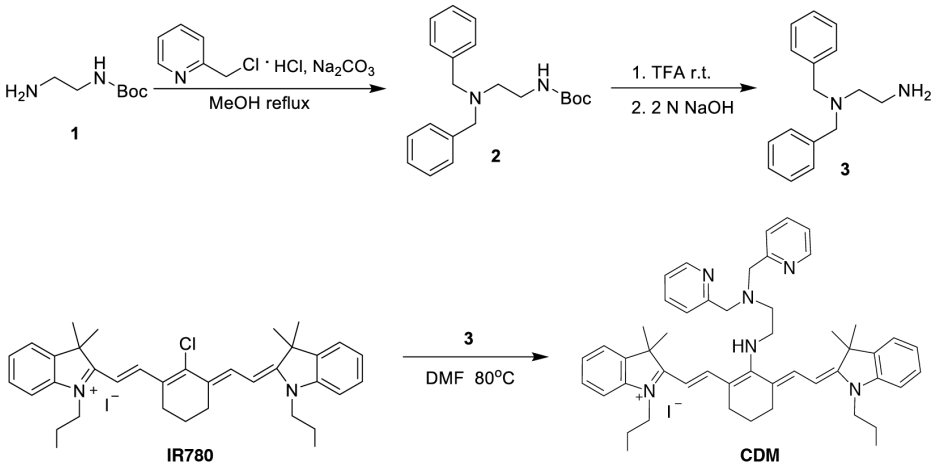

Scheme 1. Synthetic scheme of CDM.

(2) Synthesis of CDM. The last step in Scheme **1** followed reported procedures with slight modifications (Bioconjugate Chem. 1997, **8**, 751–756). Briefly, IR780 (325 mg,

0.509 mmol), compound **3** (370 mg, 1.528 mmol), and anhydrous K_2CO_3 (71 mg, 0.51 mmol) were dissolved in anhydrous DMF. The solution was heated to 80 °C and stirred for 5 h. The solvent was evaporated under reduced pressure and washed with water and brine for three times. After adding DCM, the organic layer was extracted and dried by anhydrous sodium sulfate. The crude product was purified by silica column chromatography (DCM/MeOH=50:1 to 20:1) to give final product CDM (167 mg, yield 39 %). ^{1}H NMR (400 MHz, $CDCl_3$): δ 8.44-8.42 (m, *J* = 8.0 Hz, 2H), 7.68-7.61 (m, *J* = 28.0 Hz, 4H), 7.44-7.42 (d, *J* = 8.0 Hz, 2H), 7.26-7.18 (m, *J* = 32.0 Hz, 4H), 7.14-7.11 (m, *J* = 12.0 Hz, 2H), 7.02-6.98 (t, *J* = 16.0 Hz, 2H), 6.82-6.80 (d, *J* = 8.0 Hz, 2H), 5.58-5.55 (d, *J* = 12.0 Hz, 2H), 4.02 (s, 4H), 3.82-3.73 (m, *J* = 32.0 Hz, 6H), 3.15-3.13 (m, *J* = 8.0 Hz, 2H), 2.52-2.49 (m, *J* = 12.0 Hz, 4H), 1.82-1.78 (m, *J* = 16.0 Hz, 6H), 1.56 (s, 10H), 1.24 (s, 2H), 1.03-0.99 (m, *J* = 16.0 Hz, 6H). ^{13}C NMR (100 MHz, $CDCl_3$): δ 166.49, 158.74, 149.29, 143.54, 139.97, 136.91, 128.26, 123.66, 122.52, 122.45, 122.30, 122.10, 120.16, 108.39, 93.68, 60.08, 53.81, 47.82, 47.51, 44.76, 28.93, 26.30, 21.44, 20.19, 11.98. MS: m/z calculated for $C_{50}H_{51}N_6^+$: 745.5; found: 745.5.

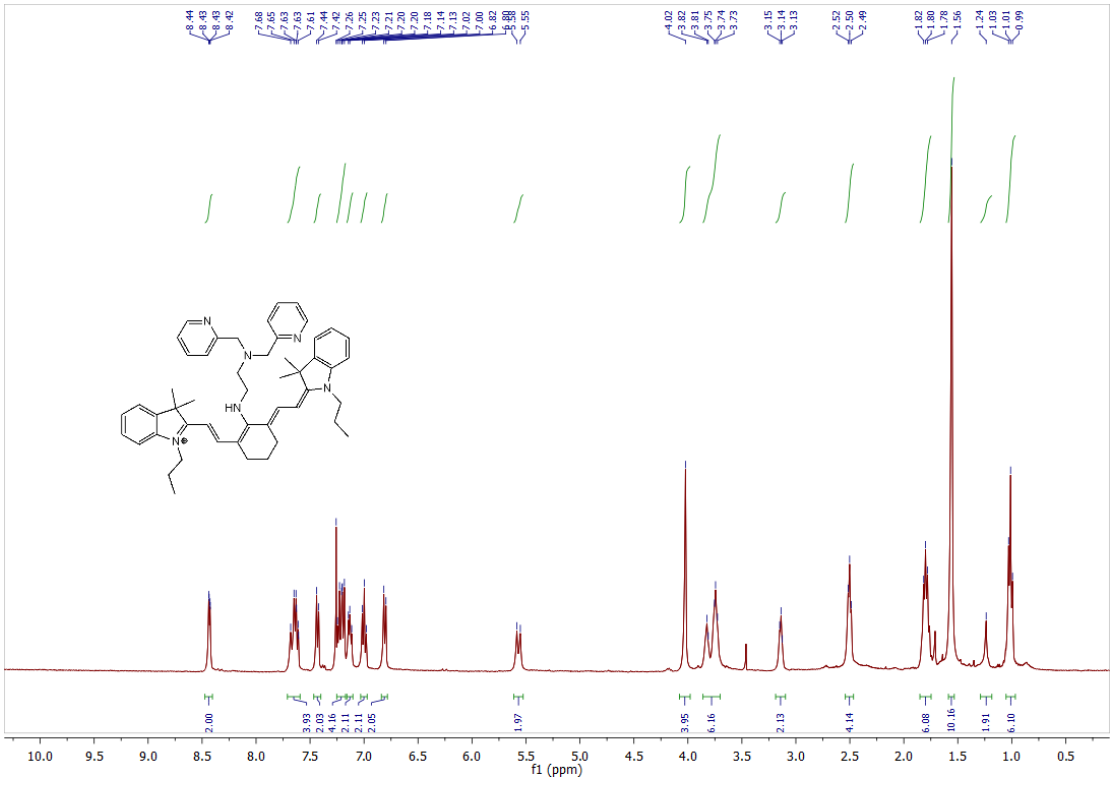

^{1}H NMR

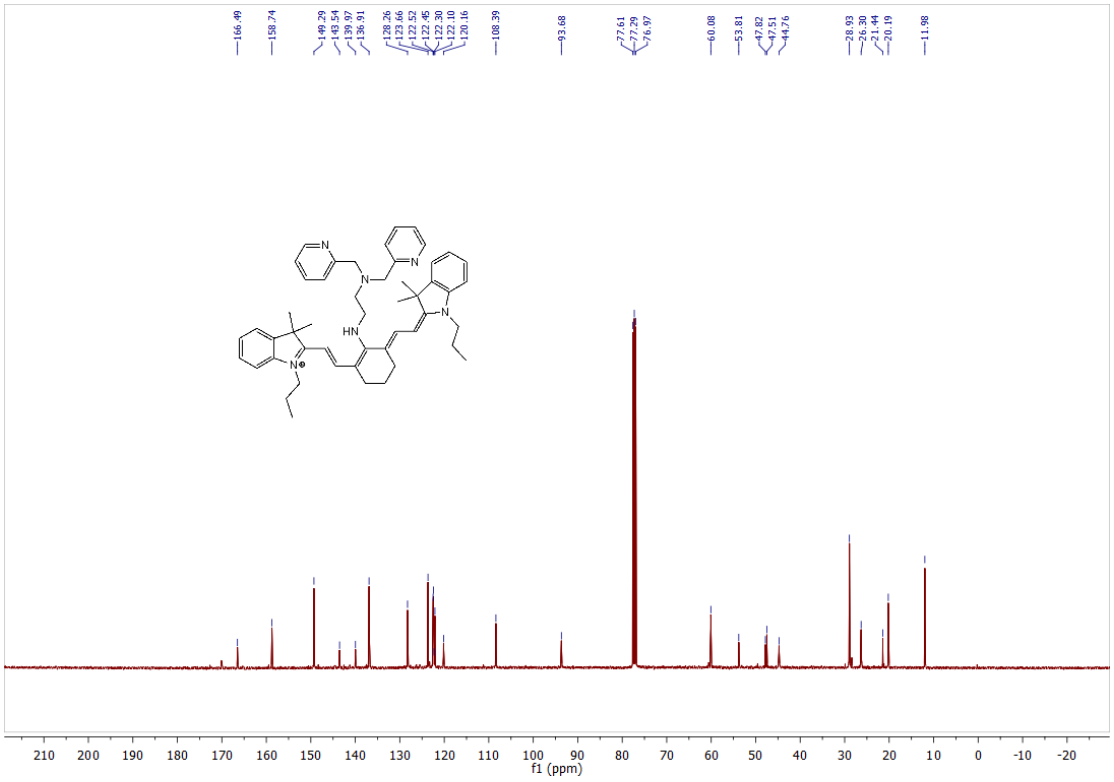

^{13}C NMR

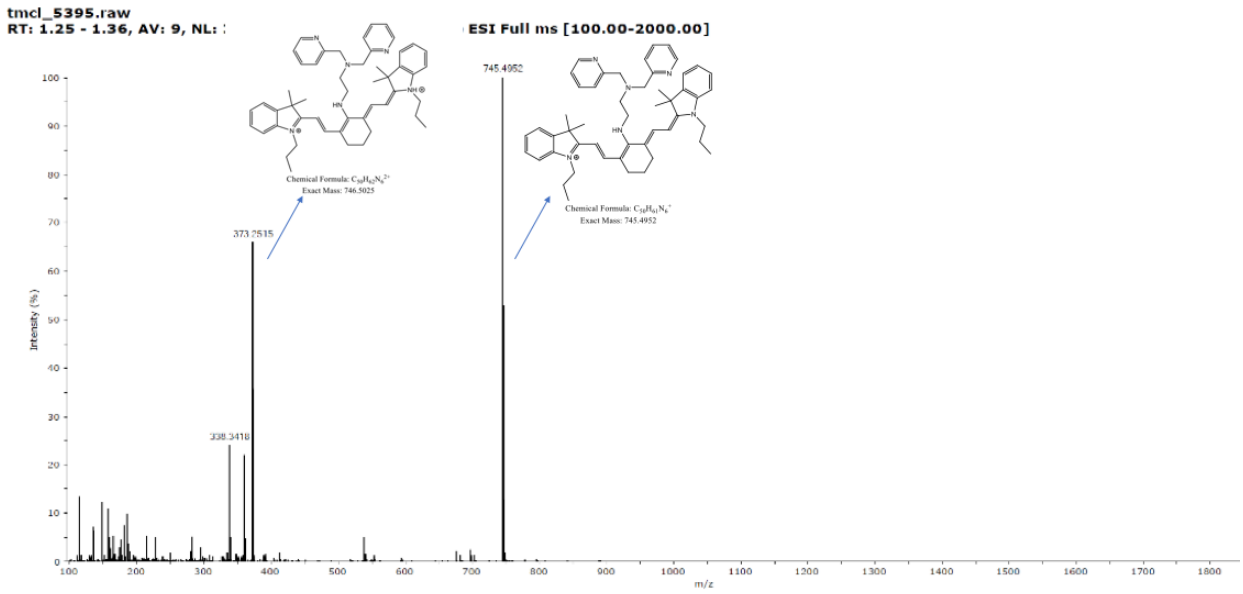

High-resolution mass spectrometry

Semiconducting polymer synthesis

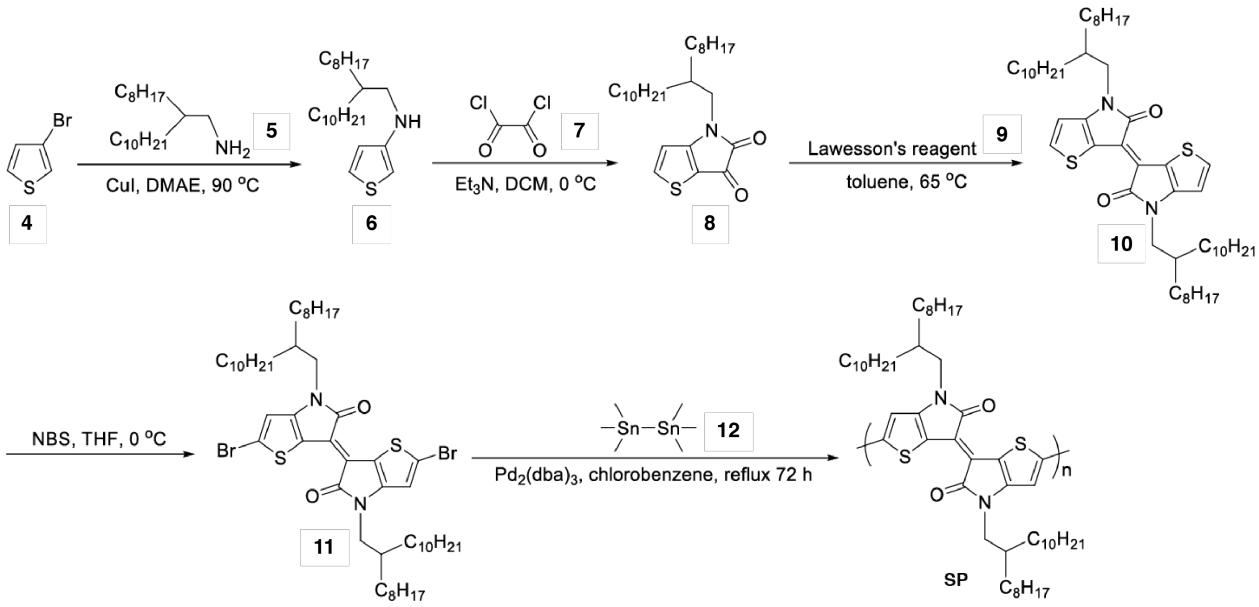

Scheme 2. Synthetic scheme of photoacoustic semiconducting polymer (SP).

(1) Synthesis of *N*-(2-octyldodecyl)thiophen-3-amine (**6**). 3-Bromothiophene (13.04 g, 80 mmol), 2-octyldodecan-1-amine (29.76 g, 100 mmol), potassium phosphate tribasic (21.23 g, 100 mmol), and copper (I) iodide (1.53 g, 8 mmol) were added into 90 mL of dimethyl aminoethanol in a 250 mL round-bottom flask, which was vacuumed and purged with argon three times, and then stirred at 90 °C for 48 h. After cooling down to room temperature, the mixture was filtered, and solvent was removed under reduced pressure. The crude product was purified by column chromatography on silica gel using ethyl acetate/hexane (*v/v* 1:10) as the eluent to afford **6** as a liquid (16.3 g, yield 43 %). ^{1}H NMR (400 MHz, $CDCl_3$, 25 °C) δ (ppm): 7.14 (d, 1H), 6.62 (d, 1H), 5.91 (d, 1H), 3.59 (br, 1H), 2.96 (d, 2H), 1.59 (br, 1H), 1.06-1.44 (m, 32H), 0.88 (m, 6H). ^{13}C NMR (100 MHz, $CDCl_3$, 25 °C) δ (ppm): 149.18, 124.95, 119.93, 94.79, 49.91, 37.84, 32.23, 31.92, 30.08, 29.66, 29.35, 26.80, 22.69, 14.11.

(2) Synthesis of 4-(2-octyldodecyl)-4*H*-thieno[3,2-*b*]pyrrole-5,6-dione (**8**). To a solution of oxalyl dichloride (6.35 g, 50 mmol) in 40 mL of dichloromethane was added dropwise a solution of compound **6** (15.19 g, 40 mmol) and 70 mL of dichloromethane at 0 °C. After 30 min, 13 mL of triethylamine in 15 mL of dichloromethane was added dropwise,

and the mixture was warmed to room temperature and stirred overnight. Then the solvents were removed under reduced pressure and the residue was purified by column chromatography on silica gel using dichloromethane/hexane (*v/v* 1:2) as the eluent to afford 4-(2-octyldodecyl)-4*H*-thieno[3,2-*b*]pyrrole-5,6-dione (**8**) as a red oil (7.8 g, yield 45%). ^{1}H NMR (400 MHz, $CDCl_3$, 25 °C) *δ* (ppm): 7.98 (d, 1H), 6.76 (d, 1H), 3.52 (d, 2H), 1.30 (br, 1H), 1.12-1.44 (m, 32H), 0.88 (m, 6H). ^{13}C NMR (100 MHz, $CDCl_3$, 25 °C) *δ* (ppm): 172.97, 165.53, 161.75, 143.77, 113.15, 111.04, 46.47, 36.98, 31.89, 31.84, 31.40, 29.89, 29.59, 29.53, 29.48, 29.31, 29.25, 26.36, 22.66, 22.64, 14.09, 14.08.

(3) Synthesis of (e)-4,4'-bis(2-octyldodecyl)-[6,6'-bithieno[3,2-*b*]pyrrolylidene]-5,5'(4*H*,4'*H*)-dione (**10**). Lawesson's reagent (3.24 g, 8 mmol) was added to a solution of compound **8** (6.51 g, 15 mmol) and 40 mL of toluene, which was vacuumed and purged with argon three times, and the mixture was stirred at 75 °C for 3 h. Then the solvent was removed under reduced pressure, and the residue was purified by column chromatography on silica gel using dichloromethane/hexane (*v/v* 1:4) as the eluent to afford **10** as a dark purple solid (4.72 g, yield 38 %). ^{1}H NMR (400 MHz, $CDCl_3$, 25 °C) *δ* (ppm): 7.51 (d, 2H), 6.78 (d, 2H), 3.69 (d, 4H), 1.89 (br, 2H), 1.05-1.43 (m, 64H), 0.87 (m, 12H). ^{13}C NMR (100 MHz, $CDCl_3$, 25 °C) *δ* (ppm): 171.30, 151.54, 134.17, 121.05, 114.25, 111.32, 46.16, 37.15, 31.91, 31.87, 31.49, 29.95, 29.61, 29.56, 29.51, 29.33, 29.27, 26.42, 22.68, 22.65, 14.11, 14.10.

(4) Synthesis of 2,2'-dibromo-4,4'-bis(2-octyldodecyl)-[6,6'bithieno[3,2,*b*]pyrrolylidene]-5,5'(4*H*,4'*H*)-dione (**11**). *N*-bromosuccinimide (2.14 g, 12 mmol) was added to compound **10** (4.18 g, 5 mmol) in 50 mL of THF at 0 °C in the absent of light. After stirred for about 2 h, the reaction mixture was poured into water and extracted with hexane. The organic layer was dried with anhydrous Na_2SO_4 and the solvent was evaporated under reduced pressure. The residue was purified by column chromatography on silica gel using dichloromethane/hexane (*v/v* 1:4) as the eluent to afford 2,2'-dibromo-4,4'-bis(2-octyldodecyl)-[6,6'bithieno[3,2,*b*]pyrrolylidene]-5,5'(4*H*,4'*H*)-dione as a dark blue solid (3.55 g, yield 71%). ^{1}H NMR (400 MHz, $CDCl_3$, 25 °C) *δ* (ppm): 6.81 (s, 2H), 3.61 (d, 4H), 1.83 (m, 2H), 1.07-1.41 (m, 64H), 0.87 (m,

12H). ^{13}C NMR (100 MHz, $CDCl_3$, 25 °C) δ (ppm): 170.32, 150.16, 123.06, 119.62, 114.94, 114.68, 46.18, 37.19, 31.92, 31.88, 31.41, 29.95, 29.63, 29.57, 29.51, 29.35, 29.29, 26.36, 22.69, 22.67, 14.11, 14.10.

(5) Synthesis of **SP.** Compound **11** (397 mg, 0.4 mmol), hexamethyldistannane (131 mg, 0.4 mmol) and dry chlorobenzene (10 mL) were added to a 50 mL of degassed and dried Schlenk tube. The solution was purged with argon for 30 min, followed by the addition of $Pd_2(dba)_3$ (20 mg), and then vacuumed and charged with argon three times. The reaction mixture was stirred vigorously at reflux for 72 h under argon atmosphere. Afterwards, the solution was poured into 300 mL of methanol and stirred for 4 h, filtered and then extracted on a Soxhlet's extractor with methanol, acetone, hexane, and chloroform successively. The final chloroform solution was concentrated, and poured into methanol, and the polymer was collected by filtration and dried under reduced pressure at room temperature for 24 h as a black solid (238 mg, yield 71%). $(C_{52}H_{86}N_2O_2S_2)_n$ $(835.39)_n$: Calcd. C, 74.76; H, 10.38; N, 3.35; O, 3.83; S, 7.68. Found C, 74.78; H, 10.36; N, 3.33; O, 3.78; S, 7.75. GPC M_n = 33.0 kDa, M_w = 76.5 kDa; PDI = 2.32.

mRNA sequencing analysis. (1) Heatmap scale (*BMC Bioinformatics,* 2010, **11**, 367), after hierarchical clustering using Median Clustering Or Weighted Pair Group Method With Centroid Averaging (WPGMC) method together with "Spearman" correlation (square of Euclidean distance) method for distance measurement on the log-transformed gene expression table, the values are further scaled in the row direction, which centers and standardizes each row separately to row Z-score.
(2) Principal-component analysis (PCA): Principal-component analysis of the populations (using around 46.7% (12328 genes in total 26475 genes) transcripts of all genes after minimal pre-filtering to keep only rows which have at least 10 read/raw counts in total). Numbers indicate frequency of transcripts described by each principal component. PCA was performed to extract the main information from the DESeq2 transformed (rlog) data set so that each successive axis was ordered by decreasing

order of variance, which plot helps to visualize the batch effects and overall effect of experimental covariates. (*Genome Biol.* 2014, **15**, 550)

(3) Distance matrix: sample-to-sample distance matrix (name of the distance matrix) indicating degree of similarity between selected cell populations calculated using (the screened transcripts (46.7%) of all genes); 12328 genes in plot indicate sample-to-sample distance. Based on the data set after differential expression analysis performed using DESeq2 measuring the effect of condition, the Euclidean distances between the samples as calculated from the rlog transformation were calculated and plotted as heatmap. (*Genome Biol.* 2014, **15**, 550)

(4) Heatmap of selected genes (genes are ordered by fold change). The selected genes were extracted from the matrix generating the general heatmap, hence the heatmaps were generated according to the normalized data set scaled in the row direction. (Renaud Gaujoux, 2014. Aheatmap: a Powerful Annotated Heatmap Engine. Package NMF-Version 0.22)

(5) The raw count table for the three conditions (Control, 15 h and 24 h) was obtained from RSEM analysis on STAR mapping. Then the normalization was performed across the samples based on the size factor (estimateSizeFactors function). The median of the ratios of observed counts was used in the following formula (*Genome Biology* 2010, **11**, R106):

$$\hat{s}j = median(i)\ \frac{k_{ij}}{\{\prod_{v=1}^{m} k_{iv}\}^{1/m}} \qquad (1)$$

where the denominator of this expression is as a pseudo-reference sample obtained by taking the geometric mean across samples and the size factor estimate $\hat{s}j$ is computed as the median of the ratios of the *j*-th sample's counts to those of the pseudo-reference.

Based on the normalized count table, the correlations between two conditions were calculated and plotted. Here, we use two comparison correlation: Ctrl vs 15hrs and Ctrl vs 24hrs. The Fold Change (15 h/Control and 24 h/Control) of 1.5 was set as cutoff threshold, and the genes with Fold Change above 1.5 are upregulated genes and the

ones with Fold Change below -1.5 are downregulated genes. Then we collected the overlapped genes between the two comparisons for upregulated and downregulated gene set separately and generate the new upregulated and downregulated gene lists. These genes lists were then fed to DAVID Functional Annotation Tool to perform GO-Term analysis. The extracted term chart was exported as the results.

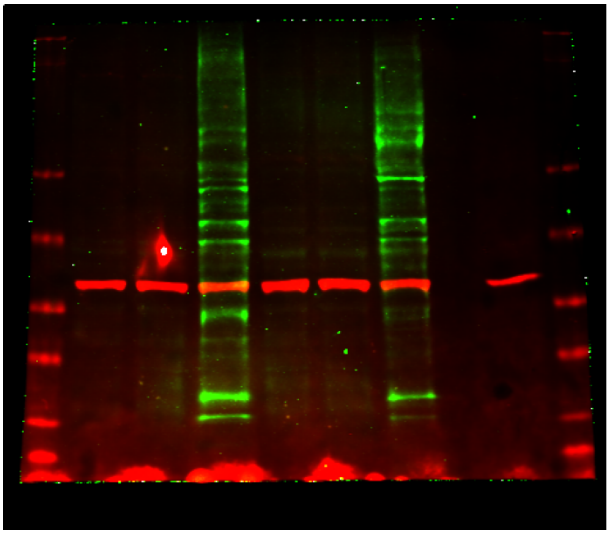

Additional Supplementary Figure 1. Unprocessed Western Blot full scan for Supplementary Figure 5a.

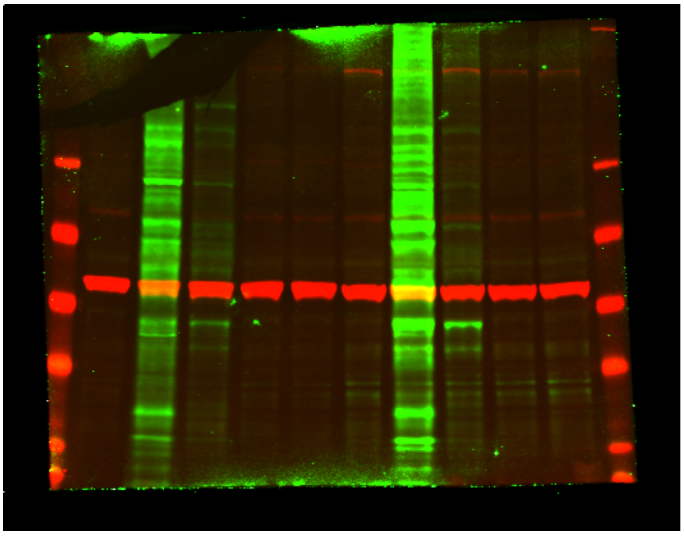

Additional Supplementary Figure 2. Unprocessed Western Blot full scan for Supplementary Figure 5b.